

# Joint Power Allocation and Splitting Control for SWIPT-enabled NOMA Systems

Jie Tang, *Senior Member, IEEE*, Yu Yu, Mingqian Liu, *Member, IEEE*, Daniel So, *Senior Member, IEEE*, Xiuyin Zhang, *Senior Member, IEEE*, Zan Li, *Senior Member, IEEE*, and Kai-Kit Wong, *Fellow, IEEE*

**Abstract**—Transmission rate and harvested energy are well-known conflictive optimization objectives in simultaneous wireless information and power transfer (SWIPT) systems, and thus their trade-off and joint optimization are important problems to be studied. In this paper, we investigate joint power allocation and splitting control in a SWIPT-enabled non-orthogonal multiple access (NOMA) system with the power splitting (PS) technique, with an aim to optimize the total transmission rate and harvested energy simultaneously whilst satisfying the minimum rate and the harvested energy requirements of each user. These two conflicting objectives make the formulated problem a constrained multi-objective optimization problem. Since the harvested power is usually stored in the battery and used to support the reverse link transmission, we transform the harvested energy into throughput and define a new objective function by summing the weighted values of the transmission rate achieved by information decoding and transformed throughput from energy harvesting, defined as equivalent-sum-rate (ESR). As a result, the original problem is transformed into a single-objective optimization problem. The considered ESR maximization problem which involves joint optimization of power allocation and PS ratio is nonconvex, and hence challenging to solve. In order to tackle it, we decouple the original nonconvex problem into two convex subproblems and solve them iteratively. In addition, both equal PS ratio case and independent PS ratio case are considered to further explore the performance. Numerical results validate the theoretical findings and demonstrate that significant performance gain over the traditional rate maximization scheme can be achieved by the proposed algorithms in a SWIPT-enabled NOMA system.

**Index Terms**—Non-orthogonal multiple access (NOMA), power splitting (PS), simultaneous wireless information and power transfer (SWIPT).

This paper was presented in part at the International Conference on Computing, Networking and Communications (ICNC), Honolulu, Hawaii, 2019. This work has been supported in part by the National Natural Science Foundation of China under Grant 61971194 and 61601186, in part by the China Scholarship Council under Grant 201806965031, in part by the Natural Science Foundation of Guangdong Province under Grant 2017A030313383, and in part by the Open Research Fund of National Mobile Communications Research Laboratory, Southeast University (No. 2019D06). (*Corresponding author: Mingqian Liu.*)

J. Tang, Y. Yu and X. Zhang are with the School of Electronic and Information Engineering, South China University of Technology, Guangzhou, China. (e-mail: eejtang@scut.edu.cn; yuyu9601@outlook.com; zhangxiuyin@scut.edu.cn).

M. Liu and Z. Li are with the State Key Laboratory of Integrated Services Networks, Xidian University, China. (e-mail: mqliu@mail.xidian.edu.cn; zanli@xidian.edu.cn).

D. K. C. So is with the School of Electrical and Electronic Engineering, University of Manchester, Manchester, United Kingdom. (e-mail: d.so@manchester.ac.uk).

K.-K. Wong is with the Department of Electronic and Electrical Engineering, University College London, London, United Kingdom. (e-mail: kai-kit.wong@ucl.ac.uk).

## I. INTRODUCTION

The rapid rise in traffic demands has driven the incentive for the research and development of the next generation of mobile networks, known as 5G [1]. Expected to be commercially available in early 2020s, 5G network will need to deliver high spectral efficiency (SE) to pave the way for future ultra high-rate applications and the Internet-of-Things (IoT) era, which aims for massive machine type communication (mMTC) and ultra-reliable low-latency communications (uRLLC). Since the conventional orthogonal multiple access (OMA) techniques are not able to meet the demand of higher SE, non-orthogonal multiple access (NOMA) has emerged as a candidate for 5G networks for its superior SE performance [2]–[4]. Unlike OMA, the key idea behind NOMA is to serve multiple users in the same resource block, i.e., time slot or subcarrier, and hence improve SE [2]. The better optimum sum rate performance for NOMA systems than OMA systems is proved with consideration of user fairness. The comparison is investigated from an optimization point of view and the advantages of NOMA over OMA was showed in practical Rayleigh fading channels. To be more practical, a downlink NOMA transmission with dynamic traffic arrival for spatially random users of different priorities was considered in [4]. By using tools from queueing theory and stochastic geometry, it was proved that the proposed NOMA scheme achieves larger stable throughput regions than OMA. The pairing between users is a problem worthy of attention in NOMA systems [5], [6]. In [5], the impact of user pairing on the performance of two NOMA systems, i.e., NOMA with fixed power allocation (F-NOMA) and cognitive-radio-inspired NOMA (CR-NOMA), has been considered. A novel low-complexity suboptimal user scheduling algorithm was proposed to maximize the system energy efficiency in [6]. Since users are sharing the same channel in NOMA system, the privacy and security in wireless networks need attention. Recently, physical-layer security has been proposed to achieve the information-theoretical security [7], [8]. In particular, the resource management scheme in [7] makes an important contribution to the field of secure communication, and the proposed analysis on the secrecy capacity and secrecy outage probability in [7], [8] provides critical guidance to the research of secure communications. In [9], cooperative jamming (CJ) was exploited to enhance the achievable secrecy energy efficiency (EE) for NOMA two-way relay wireless networks. Besides, the research on NOMA has been extended to multiple-input multiple-output (MIMO) systems [10], millimeter-wave (mmWave) communications [11] and mobile

edge computing (MEC) [12].

Meanwhile, 5G application scenarios such as blockchain based IoT ecosystem and smart city require long life battery to support the demand of high data rate services [13]. Recent progress in the research on wireless power transfer (WPT) provides the possibility of improving the lifespan of energy-constrained wireless devices [14]. Furthermore, it is known that the radio frequency (RF) signals are the carriers of both information and energy, which makes it possible to combine WPT and wireless information transmit (WIT) in wireless communications systems. Motivated by this, an advanced technology named simultaneous wireless information and power transfer (SWIPT), has emerged recently, aiming to achieve the parallel transmission of information and energy. Based on this idea, an information-theoretic study on SWIPT was first investigated in [15]. Despite being insightful, current technologies for energy harvesting are not yet able to decode the carried information directly due to the fact that the information and energy receivers sensitivities are fundamentally different, and hence such theoretical bounds are not practically feasible. Because of this, two new receiver structures were developed where information decoding (ID) and energy harvesting (EH) were separated through the time domain and the power domain, namely time switching (TS) scheme and power splitting (PS) scheme [16]. In [17], both of these practical receiving schemes have been studied in a relaying-assisted uRLLC network, where a tradeoff between the PS and TS protocols was introduced to improve the performance. With independent splitting control, the authors in [18] proposed a joint subcarrier and power allocation-based SWIPT scheme by assuming the received OFDM sub-carriers are partitioned into two groups which are used for either ID or EH. In [19], the authors considered TS-based SWIPT for a small-cell network, where the joint optimization of spatial precoding and TS ratios was addressed in order to maximize the data rates and harvested energy of all UEs simultaneously. In [20], the authors considered an EH efficiency maximization problem for both linear and non-linear model in multi-cell multiple-input single-output (MISO) networks. In [21], EE optimization was studied in MIMO two-way amplify-and-forward relay networks, where the sources, relay precoding matrices and the PS ratio are jointly optimized. Besides, SWIPT techniques have also attracted great interest in cognitive radio (CR) networks [22].

Due to the immense potential SWIPT and NOMA, the combination of these two techniques has aroused great interest. The work in [23] considered a wireless-powered NOMA communication system and focused on the joint design of downlink energy transfer and uplink information transmission. Two schemes namely the “fixed decoding order” and the “time sharing” scheme were proposed for proportional fairness improvement and individual optimization. It was demonstrated that the system performance could be significantly improved through the integration of SWIPT and NOMA. Considering the wireless powered networks are exposed to the effect of the cascaded near-far problem, the authors in [24] maximized the downlink/uplink users rate by utilizing corresponding priority weights. In addition, the cooperative NOMA scheme has been

widely used in the SWIPT-enabled NOMA system, in which near NOMA users that were close to the source acted as energy harvesting relays to help far NOMA users with poor channel conditions [25], [26]. In [25], the authors aimed at maximizing the data rate of the “strong user” while satisfying the QoS requirement of the “weak user” by jointly optimizing the PS ratios and the beamforming vectors. In [26], the performance of the cell-edge user in terms of outage probability and diversity gain was investigated with the hybrid TS/PS SWIPT NOMA architecture. The results demonstrated the achievable performance improvements of the proposed schemes in comparison to that of the OMA systems. To optimize both the SE and EE, a MISO SWIPT-enabled NOMA CR network was considered based on a non-linear EH model [27], where robust beamforming and power splitting ratio were jointly designed for minimizing the transmission power. Furthermore, an SWIPT-enabled NOMA mmWave massive MIMO system was studied in [28] where an iterative optimization algorithm was developed to maximize the achievable sum rate.

#### A. Contributions

The combination of NOMA and SWIPT is envisioned as an enabling technique to improve the SE and EE of the upcoming 5G network, and hence has drawn great interests recently. The previous literature on SWIPT-enabled NOMA systems mostly focus on achievable throughput [23], [28] or data rate for certain users [25], [26]. To satisfy the requirements of 5G scenarios, such as mMTC, the energy harvesting capacity is as important as the achievable throughput of the system. Since these two optimization objectives are conflicting to each other in SWIPT systems, the conventional method which maximizes ID rate under the EH constraint leads to energy transfer being compromised by information transmission. This is not applicable in some scenarios where energy is more valuable, such as energy demanding applications and systems that have limited access to a reliable electricity supply. Therefore, jointly optimizing the total transmission rate and the total harvested energy in SWIPT-enabled NOMA system is a problem worth investigating. Motivated by the aforementioned observations, we developed a multi-objective optimization (MOO) model for SWIPT-enabled NOMA system where we explore the efficient resource allocation strategy by jointly optimizing power allocation and splitting control, under the constraints of certain QoS requirements in terms of transmission rate and harvested energy. The main contributions of this paper can be summarized as follows.

- We developed a MOO model for SWIPT-enabled NOMA system that aim to maximize total transmission rate and total harvested energy simultaneously. The constrained MOO problem with two conflicting objectives is neither linear nor convex, and thus is extremely difficult to solve. Considering the fact that the harvested energy is usually stored in the battery and can achieve a potential capacity in the following time slots, we transform the harvested energy into throughput using Shannon formula. Then the considered MOO problem is reformulated into a single-objective optimization (SOO) problem with scalarization

method. We define a new objective function by summing the weighted values of the transmission rate achieved by ID and the transformed throughput from EH, named as “equivalent-sum-rate” (ESR).

- The corresponding ESR maximization problem which involves joint optimization of power allocation and splitting control, is still non-convex and thus very challenging to solve. In order to tackle this, we propose to decouple the transformed SOO problem into two convex subproblems and solve them iteratively via the alternating optimization algorithm. Furthermore, both equal PS ratio case (users have the same PS ratio) and independent PS ratio case (users employ different PS ratios) are considered to further explore the performance.
- Numerical results validate the theoretical findings and demonstrate that significant performance gain can be achieved by adopting the proposed algorithms, and hence prove the superiority of the integration of SWIPT technology in NOMA systems..

## B. Organization and Notation

The rest of this paper is organized as follows. The system model and the ESR optimization problem are described in Section II. In Section III, we introduce the joint power allocation and splitting control for the proposed SWIPT NOMA systems, where both equal PS ratio case and the independent PS ratio case are considered. The results of the simulations are presented in Section IV, and finally, conclusions are provided in Section VI.

The following notations are used throughout the paper. Non-bold and bold case letters represent scalar and vector respectively.

## II. SYSTEM MODEL AND PROBLEM FORMULATION

In this section, we first describe the SWIPT-enabled NOMA system model and then mathematically formulate the optimization problem.

### A. System Description

We consider a downlink NOMA system with one base station (BS) and  $N$  users. Channel state information (CSI) is assumed to be perfectly known at the BS and all the terminals. Note that the CSI at the receivers can be obtained from the channel estimation of the downlink pilots, while CSI at the transmitter can be acquired via uplink channel estimation in TDD mode. The channel power gain is denoted by  $|h_n|^2$ . Without loss of generality, the channel gains can be sorted as  $|h_1|^2 < |h_2|^2 < \dots < |h_N|^2$ . According to the principle of NOMA [29], the BS superimposes the users' messages by assigning different power which is denoted as  $p_n$  for user  $n$ . The transmit signal  $x$  can thus be expressed as

$$x = \sum_{n=1}^N \sqrt{p_n} x_n, \quad (1)$$

where  $x_n$  is the message for user  $n$ . Because the total power of BS is limited, we have the following constraint

$$\sum_{n=1}^N p_n \leq P, \quad (2)$$

where  $P$  represents the total available transmission power at the BS.

We assume that all the users are capable of harvesting energy from RF signals and perform SWIPT by applying the power splitting technique. Therefore, receivers consisting of an energy-harvesting unit and a conventional signal processing unit for concurrent EH and ID are considered in this work. Applied with PS technique, the signals sent by the BS are split into two parts: one part is used for energy harvesting, and the other part is for information conveying. Let  $\rho_n$  ( $0 \leq \rho_n \leq 1$ ) denotes the fraction of the transmission power allocated to user  $n$  for ID. And  $1 - \rho_n$  corresponds to the fraction of transmission power allocated to user  $n$  for EH. Under this setup, the signal received by the ID receiver of user  $n$  is

$$y_n^{ID} = \sqrt{\rho_n} x h_n + N_0, \quad (3)$$

where  $n_0$  represents the independent zero-mean additive white Gaussian noise (AWGN) with variance  $\sigma^2$ . With successive interference cancellation (SIC) operation, each user  $U_i$  will detect and remove the message of  $U_j$  from its observed signal, for all  $i > j$ . And for  $i < j$ , the message of user  $j$  will be treated as noise [30]. With the power split to the information receiver, the achievable transmission rate for user  $n$  can be expressed as

$$R_n^{ID} = \log_2 \left( 1 + \frac{\rho_n |h_n|^2 p_n}{\rho_n |h_n|^2 \sum_{i=n+1}^N p_i + \sigma^2} \right). \quad (4)$$

Therefore, the total transmission rate is given by

$$R_{ID} = \sum_{n=1}^N R_n^{ID}. \quad (5)$$

On the other hand, the received signal of user  $n$  for EH is given by

$$y_n^{EH} = \sqrt{1 - \rho_n} x h_n + N_0. \quad (6)$$

Here a widely accepted linear EH model [18]–[22] is considered. This assumption is reasonable due to the fact that the harvested energy is typically small in practice, which is verified in [20] that it is feasible to fit the linear EH model to the nonlinear EH model for low input power by setting the energy conversion efficiency reasonably. Besides, since the total harvested energy is one of our optimization goals in the proposed system, it is reasonable to assume that the harvested energy does not reach the receiver saturation threshold. Hence, the harvested energy at the receiver of user  $n$  is

$$e_n = \eta (1 - \rho_n) |h_n|^2 \sum_{n=1}^N p_n, \quad (7)$$

where  $\eta$  represents the energy conversion efficiency, and the noise power is very small and thus can be negligible. The total

harvested energy of the system can be written as

$$E = \sum_{n=1}^N e_n. \quad (8)$$

### B. Equivalent-Sum-Rate Optimization Problem

Our aim is to simultaneously maximize the total transmission rate and the total harvested energy. In particular, the optimization problem should be formulated considering the minimum transmission rate targets, the minimum transferred energy demands, and the total power budget. Without loss of generality, we assume the QoS requirements of each users are equivalent. Therefore, the optimization problem can be formulated mathematically as follows

$$\mathbf{P1:} \quad \max_{\mathbf{p}, \boldsymbol{\rho}} (R_{ID}(\mathbf{p}, \boldsymbol{\rho}), E(\mathbf{p}, \boldsymbol{\rho})) \quad (9a)$$

$$\text{s.t.} \quad R_n^{ID} \geq R_{min}, \quad n = 1, 2, \dots, N, \quad (9b)$$

$$e_n \geq E_{min}, \quad n = 1, 2, \dots, N, \quad (9c)$$

$$\sum_{n=1}^N p_n \leq P, \quad (9d)$$

$$\mathbf{p} > \mathbf{0}, \quad (9e)$$

$$\mathbf{0} < \boldsymbol{\rho} < \mathbf{1}. \quad (9f)$$

where  $\mathbf{p} = (p_1, p_2, \dots, p_N)^T$ ,  $\boldsymbol{\rho} = (\rho_1, \rho_2, \dots, \rho_N)^T$ ,  $R_{min}$  and  $E_{min}$  are the minimum transmission rate requirement per user and the minimum harvested energy requirement per user, respectively. There is no feasible solution if the power budget  $P$  is set to less than  $\max(P_{min}^R, P_{min}^E)$ , where  $P_{min}^R$  is the minimum power budget to satisfy the minimum transmission rate requirements and  $P_{min}^E$  is the minimum transmit power to meet the minimum harvested energy constraints. Therefore, the infeasibility is more likely happens in the case where the QoS requirements including  $R_{min}$  and  $E_{min}$  are set too high. Since we aim to maximize  $R_{ID}(\mathbf{p}, \boldsymbol{\rho})$  and  $E(\mathbf{p}, \boldsymbol{\rho})$  simultaneously, these two conflicting objectives make the formulated problem a constrained MOO problem. In general, a constrained MOO problem is defined as follows

$$\max_{\mathbf{x}} F(\mathbf{x}) = (f_1(\mathbf{x}), f_2(\mathbf{x}), \dots, f_k(\mathbf{x})) \quad (10a)$$

$$\text{s.t.} \quad g_i(\mathbf{x}) \leq 0, \quad i = 1, 2, \dots, m, \quad (10b)$$

$$h_j(\mathbf{x}) = 0, \quad j = 1, 2, \dots, n, \quad (10c)$$

where  $F(\mathbf{x})$  is the set of objective functions,  $g_i(\mathbf{x})$  is the set of inequality constraints and  $h_j(\mathbf{x})$  is the set of equality constraints. A constrained MOO problem maximizes  $k$  objective functions simultaneously, where the objective functions represent (usually) competing or conflicting objectives [31]. A MOO problem is often solved by combining its multiple objectives into a single-objective scalar function. This approach is in general known as the weighted sum or scalarization method [32]. In particular, the weighted sum method minimizes a positively weighted convex sum of the objectives, that is

$$\max_{\boldsymbol{\gamma}, \mathbf{x}} \sum_{l=1}^k \gamma_l f_l(\mathbf{x}) \quad (11a)$$

$$\text{s.t.} \quad \sum_{l=1}^k \gamma_l = 1, \quad \gamma_l > 0, \quad l = 1, 2, \dots, k, \quad (11b)$$

$$g_i(\mathbf{x}) \leq 0, \quad i = 1, 2, \dots, m, \quad (11c)$$

$$h_j(\mathbf{x}) = 0, \quad j = 1, 2, \dots, n, \quad (11d)$$

which represents a new optimization problem with a unique objective function. It can be proved that the maximizer of this SOO is an efficient solution for the original MOO [33], i.e., its image belongs to the Pareto curve. Therefore, by means of this strategy, problem **P1** can be converted to a SOO problem.

However, the unit for  $R_{ID}$  is bit/s/Hz while the unit for  $E$  is Watts, and hence it is inappropriate to directly sum them together. In practice, the harvested power is usually stored in the battery and it will be used to support the transmission in the following time slots, i.e., uplink transmission. On the basis of this, in order to unify the units of these two objective functions, we transform the harvested energy into throughput using Shannon formula, and then define a novel performance metric by summing the weighted values of the transmission rate achieved by ID and the transformed throughput from EH. Here we define  $R_n^{EH}$  to represent the achievable rate that is transformed from the harvested energy of user  $n$  as follows

$$R_n^{EH} = \log_2 \left( 1 + \frac{\zeta \eta (1 - \rho_n) |h_n|^2 \sum_{n=1}^N p_n}{\sigma^2} \right), \quad (12)$$

where  $\zeta$  denotes the efficiency converting from battery power to RF. The total data rate transformed from EH is thus given by

$$R_{EH} = \sum_{n=1}^N R_n^{EH}. \quad (13)$$

By applying this weighted sum method, the objective function of our optimization problem is converted as

$$R = \alpha R_{ID} + \gamma R_{EH}, \quad (14)$$

where  $\alpha > 0$  and  $\gamma > 0$  are the weights of the two objectives. Thus,  $R$  is the weighted sum of transmission data rate achieved by information decoding and the achievable rate that is transformed from the harvested energy. We define it as the ‘‘equivalent-sum-rate’’ (ESR), through which we evaluate the performance of the considered SWIPT-enabled system from a throughput perspective. To simplify the problem, we here normalize  $\alpha$  as 1, and  $\beta = \gamma/\alpha$ . In other words,  $\beta$  is the weight to control the service priority between ID and EH. Therefore, the objective function is rewritten as

$$R = R_{ID} + \beta R_{EH}. \quad (15)$$

When  $\beta$  is set to 0, our purpose is to maximize  $R_{ID}$  only. On the contrary, service priority is moved to energy harvesting capacity if we set  $\beta = \infty$ . Since users are required to meet their QoS demands, i.e., the minimum harvested energy requirements, the weight should satisfy  $\beta > 0$ . In addition, there is no a-priori correspondence between a weight vector and a solution vector and hence it is up to the decision maker to choose appropriate weights. Therefore, without loss of generality, we consider  $\beta$  as a constant in our optimization

problem. It should be noted that both  $R_{ID}$  and  $R_{EH}$  are non-decreasing with respect to the transmit power, and given that we aim to maximize ESR, the BS is set to use the maximum power. As a result, the transformed ESR optimization problem can be mathematically formulated as follows

$$\mathbf{P2:} \quad \max_{\mathbf{p}, \boldsymbol{\rho}} R(\mathbf{p}, \boldsymbol{\rho}) \quad (16a)$$

$$\text{s.t.} \quad R_n^{ID} \geq R_{min}, \quad n = 1, 2, \dots, N, \quad (16b)$$

$$e_n \geq E_{min}, \quad n = 1, 2, \dots, N, \quad (16c)$$

$$\sum_{n=1}^N p_n = P, \quad (16d)$$

$$\mathbf{p} > \mathbf{0}, \quad (16e)$$

$$\mathbf{0} < \boldsymbol{\rho} < \mathbf{1}. \quad (16f)$$

The considered ESR optimization problem, with joint power allocation and splitting control in the presence of inter-user interference, is non-convex. The solution is therefore non-trivial and cannot be obtained directly. In order to solve this problem, one may rely on an exhaustive search method over all the possible PS ratio and power allocation combinations. Nevertheless, it is obvious that this exhaustive search method incurs intensive computational complexity in the number of users. As a result, an efficient resource allocation strategy are developed by decomposing the optimization problem into two convex subproblems and solve them iteratively.

### III. ITERATIVE RESOURCE ALLOCATION SCHEME

In this section, we introduce the joint power allocation and splitting control algorithm for the proposed SWIPT NOMA systems. We first decouple problem **P2** into two subproblems, one is to find to the optimal PS ratio with fixed power allocation and the other is to explore the optimal power allocation scheme with fixed PS ratio. In addition, both the equal PS ratios case and the independent PS ratios case are considered to further improve the performance. These two subproblems will be proved to be convex and be solved by efficient methods. On the basis of this, we present a suboptimal algorithm for solving the original non-convex problem.

#### A. Power splitting control scheme

Here we first formulate the optimization subproblem aiming at finding the optimal PS ratio with fixed power allocation. We prove that with a fixed power allocation, the ESR  $R(\boldsymbol{\rho})$  is a concave function with respect to  $\boldsymbol{\rho}$ , and then propose an efficient algorithm to determine the power splitting ratio for each user.

1) *Independent PS Ratio Case:* Considering the independent case where the PS ratios of users are independent of each other, the corresponding subproblem with fixed power allocation can be mathematically formulated as follows

$$\mathbf{P3:} \quad \max_{\boldsymbol{\rho}} R(\boldsymbol{\rho}) \quad (17a)$$

$$\text{s.t.} \quad R_n^{ID} \geq R_{min}, \quad n = 1, 2, \dots, N, \quad (17b)$$

$$e_n \geq E_{min}, \quad n = 1, 2, \dots, N, \quad (17c)$$

$$\mathbf{0} < \boldsymbol{\rho} < \mathbf{1}, \quad (17d)$$

The Hessian matrix of  $R(\boldsymbol{\rho})$  can be expressed as

$$\frac{d^2 R(\boldsymbol{\rho})}{d\boldsymbol{\rho}^2} = \begin{bmatrix} \frac{d^2 R(\boldsymbol{\rho})}{d\rho_1^2} & \frac{d^2 R(\boldsymbol{\rho})}{d\rho_1 d\rho_2} & \dots & \frac{d^2 R(\boldsymbol{\rho})}{d\rho_1 d\rho_N} \\ \frac{d^2 R(\boldsymbol{\rho})}{d\rho_2 d\rho_1} & \frac{d^2 R(\boldsymbol{\rho})}{d\rho_2^2} & \dots & \frac{d^2 R(\boldsymbol{\rho})}{d\rho_2 d\rho_N} \\ \vdots & \vdots & \ddots & \vdots \\ \frac{d^2 R(\boldsymbol{\rho})}{d\rho_N d\rho_1} & \frac{d^2 R(\boldsymbol{\rho})}{d\rho_N d\rho_2} & \dots & \frac{d^2 R(\boldsymbol{\rho})}{d\rho_N^2} \end{bmatrix}. \quad (18)$$

Since the PS ratios of users are independent of each other, we have

$$\frac{d^2 R(\boldsymbol{\rho})}{d\rho_i d\rho_j} = 0, \quad \forall i \neq j \quad i, j = 1, 2, \dots, N. \quad (19)$$

Then the Hessian matrix of  $R(\boldsymbol{\rho})$  can be simplified as

$$\frac{d^2 R(\boldsymbol{\rho})}{d\boldsymbol{\rho}^2} = \begin{bmatrix} \frac{d^2 R(\boldsymbol{\rho})}{d\rho_1^2} & 0 & \dots & 0 \\ 0 & \frac{d^2 R(\boldsymbol{\rho})}{d\rho_2^2} & \dots & 0 \\ \vdots & \vdots & \ddots & \vdots \\ 0 & 0 & \dots & \frac{d^2 R(\boldsymbol{\rho})}{d\rho_N^2} \end{bmatrix}, \quad (20)$$

where the element  $\frac{d^2 R(\boldsymbol{\rho})}{d\rho_n^2}$  is given by (21). It is clear that  $\frac{d^2 R(\boldsymbol{\rho})}{d\rho_n^2} < 0, \forall n = 1, 2, \dots, N$ , which reveals  $\frac{d^2 R(\boldsymbol{\rho})}{d\boldsymbol{\rho}^2}$  is a negative semi-definite matrix and thus  $R(\boldsymbol{\rho})$  is a concave function with respect to  $\boldsymbol{\rho}$ . Here we rewrite the objective function as

$$\begin{aligned} R(\boldsymbol{\rho}) &= \sum_{n=1}^N R_n^{ID} + \beta \sum_{n=1}^N R_n^{EH} = \sum_{n=1}^N (R_n^{ID} + \beta R_n^{EH}) \\ &= \sum_{n=1}^N R_n, \end{aligned} \quad (22)$$

where  $R_n = R_n^{ID} + \beta R_n^{EH}$  denotes the equivalent-data-rate of user  $n$ .

Since  $\frac{d^2 R(\boldsymbol{\rho})}{d\rho_i d\rho_j} = 0, \forall i \neq j$ , the PS ratios of users are independent of each other. The maximization of the ESR for the whole system is equivalent to the maximization of individual equivalent-data-rate of each user. Consequently, problem **P3** can be divided into  $N$  parallel subproblems which can be solved using the same solution. Here we propose an efficient algorithm to solve problem **P3**. We individually maximize  $R_n(\rho_n)$  subject to the constraints of each user, and then unify a solution set from all subproblems. Generally, the subproblems of **P3** are given as follows

$$\mathbf{P4:} \quad \max_{\rho_n, n=1, 2, \dots, N} R_n(\rho_n) \quad (23a)$$

$$\text{s.t.} \quad R_n^{ID} \geq R_{min}, \quad n = 1, 2, \dots, N, \quad (23b)$$

$$e_n \geq E_{min}, \quad n = 1, 2, \dots, N, \quad (23c)$$

$$0 < \rho_n < 1. \quad (23d)$$

According to the constraints (23b)-(23d), the value of  $\rho_n$  should be limited as

$$\rho_n^{min} \leq \rho_n \leq \rho_n^{max}, \quad (24)$$

where  $\rho_n^{min} = \frac{(2^{R_{min}} - 1)\sigma^2}{|h_n|^2 p_n - (2^{R_{min}} - 1)|h_n|^2 \sum_{i=n+1}^N p_i} > 0$  ensures

$$\frac{d^2 R(\rho)}{d\rho^2} = -\frac{2\rho_n |h_n|^6 p_n \sum_{i=n}^N p_i \sum_{i=n+1}^N p_i \sigma^2 + |h_n|^4 p_n (\sum_{i=n}^N p_i + \sum_{i=n+1}^N p_i) \sigma^4}{\ln 2 (\rho_n |h_n|^2 \sum_{i=n}^N p_i + \sigma^2)^2 (\rho_n |h_n|^2 \sum_{i=n+1}^N p_i + \sigma^2)^2} - \frac{\beta \zeta^2 \eta^2 |h_n|^4 P^2}{\ln 2 (\zeta \eta (1 - \rho_n) |h_n|^2 P + \sigma^2)^2} \quad (21)$$

$$\frac{dR(\rho_n)}{d\rho_n} = \frac{|h_n|^2 p_n \sigma^2}{\ln 2 (\rho_n |h_n|^2 \sum_{i=n}^N p_i + \sigma^2) (\rho_n |h_n|^2 \sum_{i=n+1}^N p_i + \sigma^2)} + \frac{-\beta \zeta \eta |h_n|^2 P}{\ln 2 (\zeta \eta (1 - \rho_n) |h_n|^2 P + \sigma^2)} = 0, \quad (25)$$

$$\frac{dR(\rho)}{d\rho} = \sum_{n=1}^N \left( \frac{|h_n|^2 p_n \sigma^2}{\ln 2 (\rho |h_n|^2 \sum_{i=n}^N p_i + \sigma^2) (\rho |h_n|^2 \sum_{i=n+1}^N p_i + \sigma^2)} + \frac{-\beta \zeta \eta P |h_n|^2}{\ln 2 (\zeta \eta (1 - \rho) P |h_n|^2 + \sigma^2)} \right). \quad (29)$$

that the power split to ID can meet the minimum transmission rate requirement of user  $n$ , and  $\rho_n^{max} = 1 - \frac{E_{min}}{\eta |h_n|^2 P} < 1$  ensures the power fed to EH is able to satisfy the minimum harvested energy requirement. Furthermore, since  $\frac{d^2 R(\rho)}{d\rho^2} < 0, n = 1, 2, \dots, N, R_n$  is strictly concave with respect to  $\rho_n$ . It means that there is an unique root of the equation  $\frac{dR(\rho_n)}{d\rho_n} = 0$  to maximize  $R_n$ , which is expressed as (25). We denote the root as  $\hat{\rho}$ . To meet the QoS requirements, the optimal PS ratio of user  $n$  is finally given by

$$\rho_n^* = \begin{cases} \rho_n^{min}, & \hat{\rho}_n < \rho_n^{min} \\ \hat{\rho}_n, & \rho_n^{min} \leq \hat{\rho}_n \leq \rho_n^{max} \\ \rho_n^{max}, & \hat{\rho}_n > \rho_n^{max} \end{cases}. \quad (26)$$

Thus the optimal solution of **P3** is  $\rho^* = (\rho_1^*, \rho_2^*, \dots, \rho_N^*)^T$ .

2) *Equal PS Ratio Case*: We also consider the special case that all users share the same PS ratio. Based on this setup, the subproblem to obtain the optimal common PS ratio with fixed power allocation is simplified as follows

$$\mathbf{P5}: \quad \max_{\rho} R(\rho) \quad (27a)$$

$$\text{s.t. } R_n^{ID} \geq R_{min}, \quad \forall n = 1, 2, \dots, N, \quad (27b)$$

$$e_n \geq E_{min}, \quad \forall n = 1, 2, \dots, N, \quad (27c)$$

$$0 < \rho < 1. \quad (27d)$$

According to the constraints (27b)-(27d), the value of  $\rho$  should satisfy the following condition

$$\rho_n^{min} \leq \rho \leq \rho_n^{max}, \quad \forall n = 1, 2, \dots, N. \quad (28)$$

With equal PS ratio  $\rho$  among users, it is easy to prove (27a) is a concave function of  $\rho$  due to the property of weighted sum of logarithm functions. Therefore, similar to the process to get the optimal independent PS ratios, we obtain the optimal unified  $\rho$  by setting  $\frac{dR(\rho)}{d\rho} = 0$ . The root of this equation that meet the constraints (27b)-(27d) is the optimal solution, and is referred to as  $\hat{\rho}_e$ . The expression of  $\frac{dR(\rho)}{d\rho}$  is detailed given by (29). If  $\hat{\rho}_e$  is beyond the range of (28), it reveals that  $\hat{\rho}_e$  can not meet all the QoS constraints. In this case, the optimal PS ratio is set to the minimum or the maximum value that are limited by all the constraints in (27b)-(27c). To summarize,

the strategy in equal PS ratio case is given by

$$\rho_e^* = \begin{cases} \rho_e^{min}, & \hat{\rho}_e < \rho_n^{min} \\ \hat{\rho}_e, & \rho_e^{min} \leq \hat{\rho}_e \leq \rho_e^{max} \\ \rho_e^{max}, & \hat{\rho}_e > \rho_n^{max} \end{cases}, \quad (30)$$

where  $\rho_e^{min} = \max(\rho_n^{min}), \forall \hat{\rho}_e < \rho_n^{min}$  and  $\rho_e^{max} = \min(\rho_n^{max}), \forall \hat{\rho}_e > \rho_n^{max}$ .

## B. Power allocation scheme

In this section, we first prove that with fixed PS ratios, the ESR  $R(\mathbf{p})$  is a concave function in  $\mathbf{p}$ . Based on this result, we propose an efficient power allocation algorithm to solve the corresponding subproblem, which can be mathematically formulated as follows

$$\mathbf{P6}: \quad \max_{\mathbf{p}} R(\mathbf{p}) \quad (31a)$$

$$\text{s.t. } R_n^{ID} \geq R_{min}, \quad n = 1, 2, \dots, N, \quad (31b)$$

$$\sum_{n=1}^N p_n = P, \quad (31c)$$

$$\mathbf{p} > \mathbf{0}. \quad (31d)$$

To solve the above problem, a relationship between ESR  $R(\mathbf{p})$  and the power allocation  $\mathbf{p}$  is derived as in the following proposition.

**Proposition 1.** *With fixed transmit power and PS ratios, the objective function of problem **P6** is a concave function with respect to  $\mathbf{p}$  if and only if  $\rho_1 |h_1|^2 \leq \rho_2 |h_2|^2 \leq \dots \leq \rho_N |h_N|^2$ .*

Proof: see Appendix A.

Here we assume  $\rho_1 |h_1|^2 < \rho_2 |h_2|^2 < \dots < \rho_N |h_N|^2$ , and then the objective function of **P4** is concave according to **Proposition 1**. Since (31b) is convex and (31c), (31d) are linear, problem **P6** is convex, which can be solved by standard numerical methods such as interior point method. Although the convex programming approach is numerically stable, however, its computational complexity depends on the number of optimizing variables, which can be problematic if the number of users is large. Therefore, to reduce the complexity, we use Lagrange dual decomposition method

which is more efficient. The Lagrangian function is given by

$$\mathcal{L}(\mathbf{p}, \boldsymbol{\lambda}, \mu) = -R(\mathbf{p}) + \sum_{n=1}^N \lambda_n f_n + \mu h, \quad (32)$$

where  $\boldsymbol{\lambda} = (\lambda_1, \lambda_2, \dots, \lambda_N)^T$  is the Lagrange multiplier vector with elements  $\lambda_n \geq 0$  corresponds to the constraints in (31b),  $\mu \geq 0$  is the Lagrange multiplier corresponds to the constraint (31c), and

$$f_n = R_{min} - \log_2 \left( 1 + \frac{\rho_n |h_n|^2 p_n}{\rho_n |h_n|^2 \sum_{i=n+1}^N p_i + \sigma^2} \right), \quad (33)$$

$$h = \sum_{n=1}^N p_n - P. \quad (34)$$

The Karush-Kuhn-Tucker (KKT) conditions of problem **P6** is given by

$$\frac{d\mathcal{L}(\mathbf{p}, \boldsymbol{\lambda}, \mu)}{dp_n} = 0, \quad \forall n = 1, 2, \dots, N, \quad (35a)$$

$$f_n \leq 0, \quad \forall n = 1, 2, \dots, N, \quad (35b)$$

$$h = 0, \quad (35c)$$

$$\lambda_n f_n = 0, \quad \forall n = 1, 2, \dots, N, \quad (35d)$$

$$\mu h = 0, \quad (35e)$$

$$\lambda_n \geq 0, \quad \forall n = 1, 2, \dots, N, \quad (35f)$$

$$\mu \geq 0, \quad (35g)$$

and for a given user  $\bar{n}$ ,  $\frac{d\mathcal{L}(\mathbf{p}, \boldsymbol{\lambda}, \mu)}{dp_{\bar{n}}}$  is detailed as (36).

According to (35a), we obtain  $\frac{d\mathcal{L}(\mathbf{p}, \boldsymbol{\lambda}, \mu)}{dp_n} - \frac{d\mathcal{L}(\mathbf{p}, \boldsymbol{\lambda}, \mu)}{dp_{n-1}} = 0$ , which is analyzed in (37). Then we have

$$\begin{aligned} & \frac{\lambda_{n-1} \rho |h_{n-1}|^2}{\ln 2 (\rho |h_{n-1}|^2 \sum_{i=n-1}^N p_i + \sigma^2)} - \frac{\lambda_n \rho |h_n|^2}{\ln 2 (\rho |h_n|^2 \sum_{i=n}^N p_i + \sigma^2)} \\ &= \frac{\rho |h_n|^2}{\ln 2 (\rho |h_n|^2 \sum_{i=n}^N p_i + \sigma^2)} - \frac{\rho |h_{n-1}|^2}{\ln 2 (\rho |h_{n-1}|^2 \sum_{i=n}^N p_i + \sigma^2)} \\ &> 0. \end{aligned} \quad (38)$$

With  $\rho_1 |h_1|^2 < \rho_2 |h_2|^2 < \dots < \rho_N |h_N|^2$ , it is easy to obtain  $\lambda_n > 0$  when  $n = 1, 2, \dots, N - 1$ . Under the constraint of (35d), the constraints of (31b) hold with equality for  $n = 1, 2, \dots, N - 1$ . With  $\lambda_N > 0$ ,  $f_N = R_{min} - \log_2 \left( 1 + \frac{\rho_N p_N |h_N|^2}{\sigma^2} \right) = 0$ . In this case, all the users' achievable transmission rates are just satisfying the minimum QoS requirements. Thus, we can calculate the corresponding total power consumption, denoted as  $P_{min}$ , which indicates the minimum power needed to satisfy all users' minimum QoS requirements. Hence, we suppose  $P \geq P_{min}$  in this work for a practical configuration. With  $\lambda_N = 0$ ,  $f_N$  can be negative, it demonstrates that the achievable transmission rate of the user with best channel gain can further improve under the premise of meeting the minimum rate requirements. This is critical to the improvement of system's throughput.

For the case that  $P = P_{min}^R$ , to obtain the optimal power

allocation, we only need to set  $R_n^{ID} = R_{min}$  for all the users, and  $p_n$  can be sequentially determined in the order  $n = N, N - 1, \dots, 1$ .

For the case that  $P > P_{min}^R$ , the constraints in (31b) hold with equality for  $n = 1, 2, \dots, N - 1$  except  $n = N$ . Hence, under the premise of satisfying the minimum data rate requirements of the first  $N - 1$  users with poor channel conditions, the BS transmits to the user with the best channel using the remaining power  $P - \sum_{i=1}^{N-1} p_i$ . Therefore, we can conclude the optimal power allocation solution for problem **P6** as

$$\begin{cases} p_n = \frac{2^{R_{min}-1}}{2^{R_{min}}} \left( P - \sum_{i=1}^{n-1} p_i + \frac{\sigma^2}{\rho_n |h_n|^2} \right), n = 1, 2, \dots, N - 1 \\ p_N = P - \sum_{n=1}^{N-1} p_n \end{cases} \quad (39)$$

The proposed power allocation scheme indicates that more resources are allocated to the user with best channel condition in order to further improve the system, and similar results are observed in the conventional NOMA systems [34].

### C. Joint Optimization of Power Allocation and Power Splitting Ratio

The ESR optimization problem **P2**, with joint power allocation and splitting control in the presence of inter-user interference, is non-convex. The solution is therefore non-trivial and cannot be obtained directly. As stated in [35], for any optimization problems with multiple variables, we can analyze and solve the problem over some variables, regarding the rest as constants; and then solve the problem over the remaining variables. Therefore, we will separate  $\mathbf{p}$  and  $\boldsymbol{\rho}$  when developing the optimization algorithm so as to overcome the difficulty. In other words, on the basis that the objective function is concave on  $\mathbf{p}$  and  $\boldsymbol{\rho}$  respectively, we are able to find an efficient solution by solving the two subproblems iteratively, as described in Section III.A and III.B.

In this work, both equal PS ratio case and independent PS ratios case are considered. For the case of equal PS ratio, we randomly generate a PS ratio  $\rho$  and then obtain the optimal power allocation scheme according to (39) first. Then we determine the optimal PS ratio using (30) with  $\mathbf{p}$  obtained in the previous step. Since  $\rho |h_1|^2 < \rho |h_2|^2 < \dots < \rho |h_N|^2$  and the objective function can be proved to be concave over  $\mathbf{p}$  in this case, the equivalent-sum-rate will be increased after each iteration until achieving the maximum, i.e., the ESR cannot be further improved. Since the optimal PS ratio and power allocation are calculated directly from (30) and (39), the involved complexity are  $O(1)$  and  $O(N)$  respectively. According to [36], the computational complexity method with stopping criteria  $\delta$  is  $O(\frac{1}{\delta^2} \log(N))$ . Thus the overall computational complexity of this algorithm is  $O(\frac{1}{\delta^2} N \log(N))$ .

For the case of independent PS ratio, we begin with finding the optimal PS ratios. We first initialize the PS ratio of each user with arbitrary value and determine the power allocation according to (39). With fixed  $\mathbf{p}$ , we can obtain

$$\begin{aligned} \frac{d\mathcal{L}(\mathbf{p}, \boldsymbol{\lambda}, \mu)}{dp_{\bar{n}}} &= \sum_{n=1}^{\bar{n}-1} \lambda_n \frac{\rho_n^2 |h_n|^4 p_n}{\ln 2 (\rho_n |h_n|^2 \sum_{i=n}^N p_i + \sigma^2) (\rho_n |h_n|^2 \sum_{i=n+1}^N p_i + \sigma^2)} - \lambda_{\bar{n}} \frac{\rho_{\bar{n}} |h_{\bar{n}}|^2}{\ln 2 (\rho_{\bar{n}} |h_{\bar{n}}|^2 \sum_{i=\bar{n}}^N p_i + \sigma^2)} \\ &\quad - \sum_{n=1}^{\bar{n}-1} \left( \frac{\rho_{n+1} |h_{n+1}|^2}{\ln 2 (\rho_{n+1} |h_{n+1}|^2 \sum_{i=n+1}^N p_i + \sigma^2)} - \frac{\rho_n |h_n|^2}{\ln 2 (\rho_n |h_n|^2 \sum_{i=n+1}^N p_i + \sigma^2)} \right) - \frac{\rho_1 |h_1|^2}{\ln 2 (\rho_1 |h_1|^2 \sum_{i=1}^N p_i + \sigma^2)} + \mu. \end{aligned} \quad (36)$$

$$\begin{aligned} \frac{d\mathcal{L}(\mathbf{p}, \boldsymbol{\lambda}, \mu)}{dp_n} - \frac{d\mathcal{L}(\mathbf{p}, \boldsymbol{\lambda}, \mu)}{dp_{n-1}} &= \frac{\rho_{n-1} |h_{n-1}|^2}{\ln 2 (\rho_{n-1} |h_{n-1}|^2 \sum_{i=n}^N p_i + \sigma^2)} - \frac{\rho_n |h_n|^2}{\ln 2 (\rho_n |h_n|^2 \sum_{i=n}^N p_i + \sigma^2)} \\ &\quad + \frac{\lambda_{n-1} \rho_{n-1} |h_{n-1}|^2}{\ln 2 (\rho_{n-1} |h_{n-1}|^2 \sum_{i=n-1}^N p_i + \sigma^2)} - \frac{\lambda_n \rho_n |h_n|^2}{\ln 2 (\rho_n |h_n|^2 \sum_{i=n}^N p_i + \sigma^2)}, \end{aligned} \quad (37)$$

TABLE I: THE PROPOSED SUBOPTIMAL RESOURCE ALLOCATION ALGORITHM WITH EQUAL PS RATIO

- I. Randomly initial PS ratio  $\rho^{(1)}$ ,  $0 < \rho^{(1)} < 1$ , set  $R_{\rho}^{(1)} = NR_{min} + \beta N \log_2(1 + \frac{\zeta E_{min}}{\sigma^2})$ ,  $\delta = 10^{-5}$  as the maximum tolerance;
- II. Solve the problem **P6** using (39) with  $\rho^{(1)}$ , record the power allocation as  $\mathbf{p}^{(1)}$  and ESR as  $R_{\rho}^{(1)}$ ;
- III. **REPEAT**  
Solve the problem **P5** using (29)(30) with  $\mathbf{p}^{(t-1)}$ , record the common PS ratio as  $\rho^{(t)}$  and ESR as  $R_{\rho}^{(t)}$ ,  
**IF**  $R_{\rho}^{(t)} - R_{\rho}^{(t-1)} > \delta$ :  
Solve the problem **P6** using (39) with  $\rho^{(t)}$ , record the power allocation as  $\mathbf{p}^{(t)}$  and ESR as  $R_{\rho}^{(t)}$ ;  
**IF**  $R_{\rho}^{(t)} - R_{\rho}^{(t-1)} > \delta$ :  
Convergence = **FALSE**;  
**ELSE**  
Convergence = **TRUE**, **RETURN**  $\mathbf{p}^* = \mathbf{p}^{(t-1)}$ ,  
 $\rho^* = \rho^{(t)}$ ,  $R^* = R_{\rho}^{(t)}$ ;  
**END**  
**ELSE**  
Convergence = **TRUE**, **RETURN**  $\mathbf{p}^* = \mathbf{p}^{(t-1)}$ ,  
 $\rho^* = \rho^{(t-1)}$ ,  $R^* = R_{\rho}^{(t-1)}$ ;  
**END**  
**UNTIL** Convergence = **TRUE**.

TABLE II: THE PROPOSED SUBOPTIMAL RESOURCE ALLOCATION ALGORITHM WITH INDEPENDENT PS RATIO

- I. Randomly initial PS ratio  $\rho^{(1)}$ ,  $0 < \rho_n^{(1)} < 1, n = 1, 2, \dots$ ,  $N$ , set  $R_{\rho}^{(1)} = NR_{min} + \beta N \log_2(1 + \frac{\zeta E_{min}}{\sigma^2})$ ,  $\delta = 10^{-5}$  as the maximum tolerance;
- II. Solve the problem **P6** using (39) with  $\rho^{(1)}$ , record the power allocation as  $\mathbf{p}^{(1)}$  and ESR as  $R_{\rho}^{(1)}$ ;
- III. **REPEAT**  
Solve the problem **P4** using (25)(26) with  $\mathbf{p}^{(t-1)}$ , record the PS ratio as  $\rho^{(t)}$  and ESR as  $R_{\rho}^{(t)}$ , reorder  $\rho_n^* |h_n|^2$  in the ascending order;  
**IF**  $R_{\rho}^{(t)} - R_{\rho}^{(t-1)} > \delta$ :  
Solve the problem **P6** using (39) with  $\rho^{(t)}$ , record the power allocation as  $\mathbf{p}^{(t)}$  and ESR as  $R_{\rho}^{(t)}$ ;  
**IF**  $R_{\rho}^{(t)} - R_{\rho}^{(t-1)} > \delta$ :  
Convergence = **FALSE**;  
**ELSE**  
Convergence = **TRUE**, **RETURN**  $\mathbf{p}^* = \mathbf{p}^{(t-1)}$ ,  
 $\rho^{(*)} = \rho^{(t)}$ ,  $R^* = R_{\rho}^{(t)}$ ;  
**END**  
**ELSE**  
Convergence = **TRUE**, **RETURN**  $\mathbf{p}^* = \mathbf{p}^{(t-1)}$ ,  
 $\rho^{(*)} = \rho^{(t-1)}$ ,  $R^* = R_{\rho}^{(t-1)}$ ;  
**END**  
**UNTIL** Convergence = **TRUE**.

the optimal PS ratios with (25) and (26). Before going onto the next step to find the optimal power allocation, we multiply the optimal PS ratios with the corresponding channel gains and reordering them in ascending order, such that the proposed approach for subproblem **P6** is feasible. The two subproblems will be solved iteratively until the ESR converges. Since the PS ratios are different for each user, the computational complexity of the proposed PS splitting control scheme is  $O(N)$ . Here we use the bubble sorting algorithm to reorder  $\rho_n^* |h_n|^2$  and the involved complexity is  $O(N)$ . Therefore, the overall computational complexity is given by  $O(\frac{1}{\delta^2} N^3 \log(N))$ , which is higher than the identical case.

The complete algorithms to solve the optimization problem

for SWIPT NOMA systems with the PS technique are summarized in Table I and Table II.

#### IV. SIMULATION RESULTS AND DISCUSSION

In this section, simulation results are provided in order to validate the performance of the proposed joint power allocation and splitting control algorithms in the SWIPT-enabled NOMA systems. It is assumed that six users are uniformly-distributed in the coverage area of BS within 20m. All the results are obtained from various random locations of the users. Both the large scale fading model and small



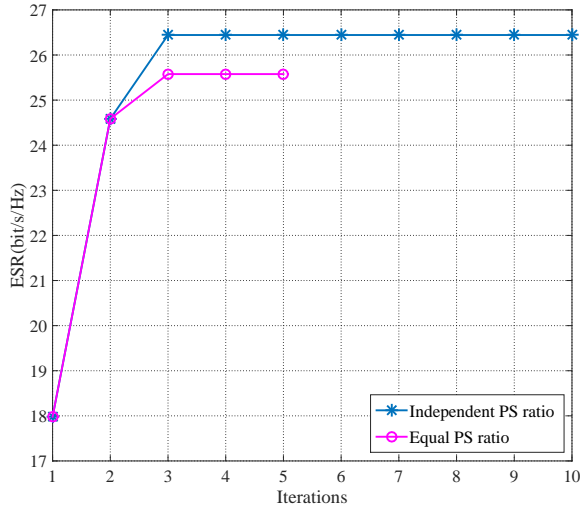


Fig. 1: Convergence performance of the proposed joint power allocation and splitting control algorithms.

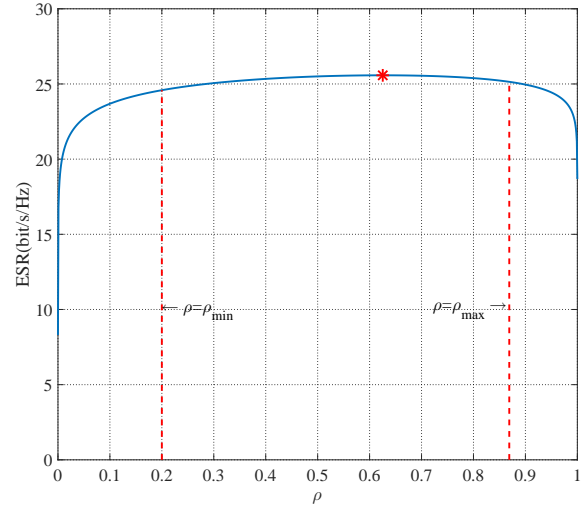


Fig. 2: ESR versus PS ratio under fixed power allocation (equal PS ratio).

scale fading model are considered. The former is given by  $128.1 + 37.6 \log_{10} d$ , in which  $d$  is the distance between the users and the BS in  $km$ . Besides, Log-Normal shadowing with standard deviation of  $8dB$  is considered [37]. For the small-scale fading, each terminal experiences independent Rayleigh fading with unit variance. In other words, the small-scale fading is an independent and identically distributed zero mean circularly symmetric complex Gaussian (ZMCSCG) random variable with variance of 1. In addition, the EH efficiency  $\eta$  is set to 0.6 [38], the conversion efficiency  $\zeta$  is set to 10%, and the preference coefficient (combining weights)  $\beta$  is set to 0.1. The power budget is set to  $P = 5W$ . In order to guarantee QoS requirements for each user, the minimum transmission rate constraint per user is set to 2 bit/s/Hz, and the minimum harvested energy per user is set to 0.1 mW. Note that, in all our simulations, if any user whose transmission rate or harvested energy does not meet the requirements, the ESR is set to zero. Furthermore, it should be noted that these system parameters are merely chosen to demonstrate the performance in an example and can easily be modified to any other values depending on the specific scenario under consideration.

In the first simulation, the convergence performance of the proposed joint power allocation and splitting control algorithms is studied. In particular, both the equal PS ratio case and the independent PS ratio case are investigated. As shown in Fig. 1, it can be observed that the ESR of both cases converge to a stable value. Furthermore, it is clear that the latter one can achieve higher performance gains in terms of ESR, but at the cost of higher computational complexity.

We then evaluate the relationship between the ESR and the PS ratio. The results in Fig. 2 and Fig. 3 is in line with our theoretical analysis where both the ESR (with respect to equal PS ratio  $\rho$ ) and the equivalent-data-rate (with respect to independent PS ratio  $\rho_n$ ) are concave. Since information and energy are transmitted through the same signal, there is a trade-off between the achievable data rate and harvested energy. Thus, given the fact that the ESR is defined as the

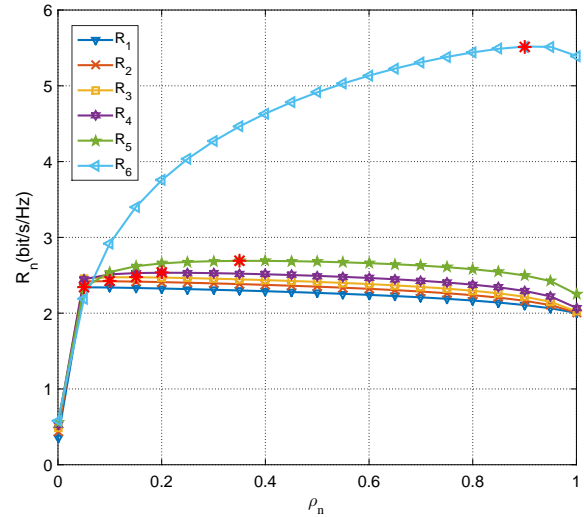


Fig. 3: Equivalent-data-rate versus PS ratio under fixed power allocation (independent PS ratio).

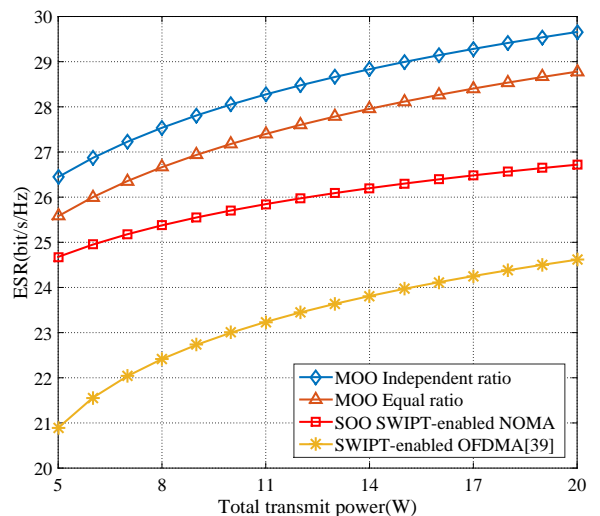


Fig. 4: ESR versus total transmit power.

weighted sum of  $R_{ID}$  and  $R_{EH}$ , there exists an optimum value for simultaneous optimization of throughput and harvested energy. It can be seen in Fig. 2 that there exists a maximum value between  $\rho_{min}$  and  $\rho_{max}$  for the equal PS case, and this confirms that the PS ratio obtained according to our proposed scheme is unique and optimal. For the independent PS ratio case, the equivalent-data-rate of the first  $N - 1$  users change slowly as  $\rho_n$  increases while the  $N^{th}$  user's equivalent-data-rate is significantly affected. The reason for this observation is that the inter-user interference among NOMA users leads to an imbalanced allocation of resources, while the  $N^{th}$  user, which gets all the remaining energy and without interference, has the best performance that significantly affected by  $\rho_n$ . Fig. 3 further reveals that the optimal independent PS ratio increases as the channel condition improves, which coincides with the precondition  $\rho_1|h_1|^2 < \rho_2|h_2|^2 < \dots < \rho_N|h_N|^2$  and guarantees the concavity of the objective function of **P4** when users employ independent PS ratio.

In the next simulation, the performance of the proposed schemes is evaluated under different power budgets. In order to valid the effectiveness of the proposed MOO model, we apply the conventional method where the ID rate is maximized under the EH constraint in the considered system, marked as "SOO SWIPT-enabled NOMA". In addition, the performance of conventional SWIPT-enabled OFDMA system [39] is also presented for comparison, marked as "SWIPT-enabled OFDMA". In SWIPT-enabled OFDMA system, each user occupies the channel exclusively and the power splitting control is independent of each other. It has been shown in Fig. 4 that the ESR achieved by all the approaches are monotonically increasing in the total transmit power. Particularly, it has been shown that our proposed MOO-based solution with independent PS ratio is capable of providing extra gains (in terms of ESR) compared to the conventional algorithm that only maximizes the transmission rate. For the conventional algorithm, the power transfer needs to be compromised for information transmission, such that the optimum allocation of the resources is shifted to those maximize the sum data rate. In contrast, the proposed MOO algorithm considers the balance between information transmission and energy harvesting, and can achieve better system performance. And it is clear that the performance achieved by all the SWIPT-NOMA schemes outperform the SWIPT-OFDMA scheme, which has confirmed the advantages of combination of SWIPT and NOMA. In addition, the proposed algorithm with independent PS ratio outperforms the one with equal PS ratio due to diversity gain. This can be observed in Fig. 3 that the optimal PS ratio is different for each user, and hence the sharing PS ratio method limits the improvement of system performance.

We then analyse the impact of number of users to the maximum ESR by setting the number of users to 4, 6 and 8. As it can be seen in Fig. 5, the ESR increases with the number of users when the total transmit power is sufficiently large. This is because a higher diversity gain is offered when more users are served simultaneously. On the other hand, with small transmit power, ESR becomes zero with increasing number of users. In fact, the non-orthogonality of the channel access is the main reason for this observation. In NOMA systems,

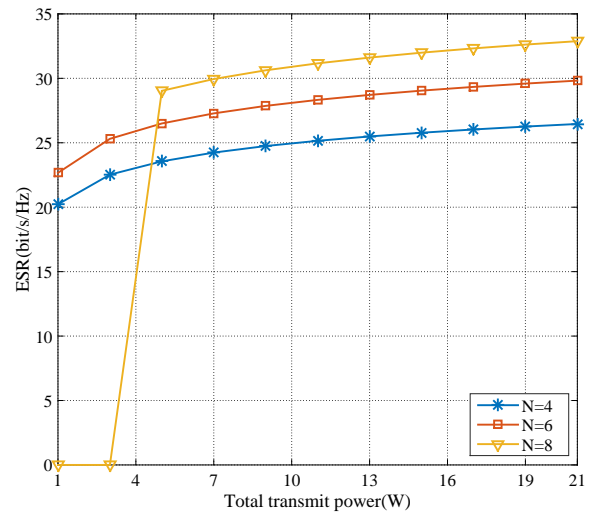


Fig. 5: ESR versus total transmit power with different number of users.

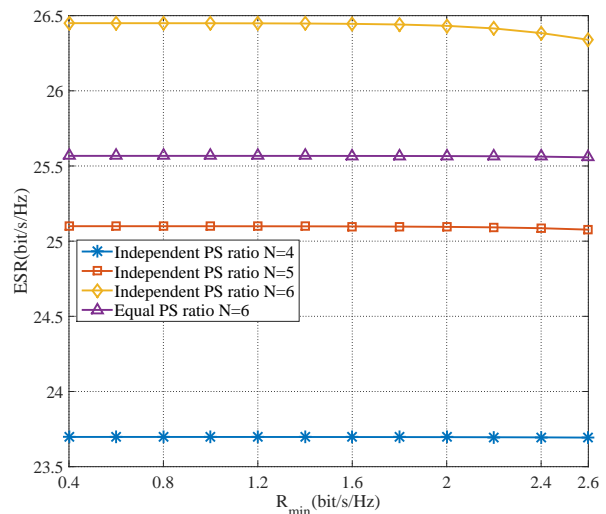


Fig. 6: ESR versus minimum transmission rate requirement per user.

the inter-user interference would enhance with the increasing number of terminals. This reveals that a considerably higher transmit power is needed so as to achieve the minimum rate requirement for each terminal. In other words, limited transmit power can not meet the minimum transmission rate requirements of all the users. Therefore, there exists a trade-off between ESR performance and the number of users, especially for the system with limited power.

In the next simulations, we analyse the impact of the minimum transmission rate and minimum harvested energy requirements to ESR in different cases. The impact of the number of users as well as difference splitting strategies are also considered. The number of users is set to 4, 5 and 6. As it can be seen from Fig. 6 and Fig. 7, the ESR remains nearly unchanged up to a particular minimum transmission rate or harvested energy constraints, but decreases thereafter. This is because that when QoS requirements are sufficiently small, the resource allocation is sufficient to guarantee the

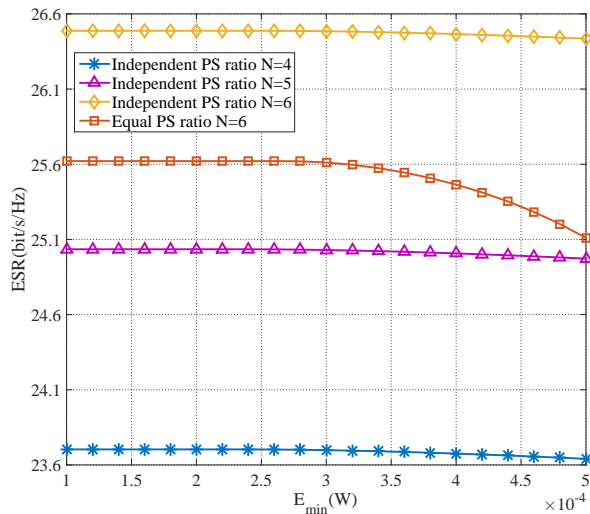


Fig. 7: ESR versus minimum harvested energy requirement per user.

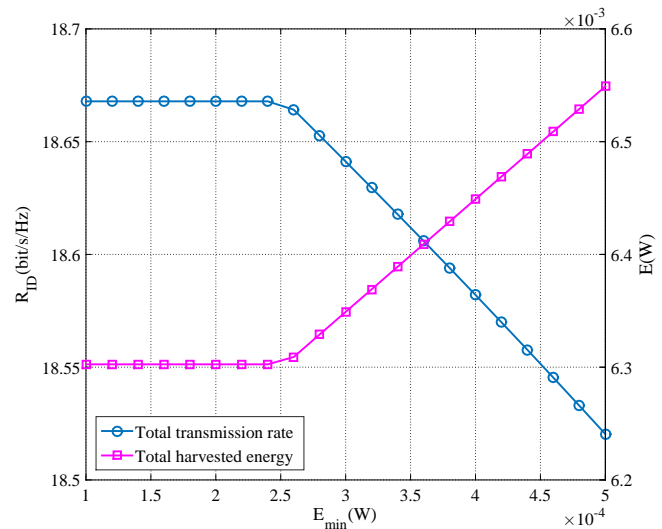


Fig. 9: Total transmission rate and harvested energy versus minimum harvested energy requirement with independent PS ratio

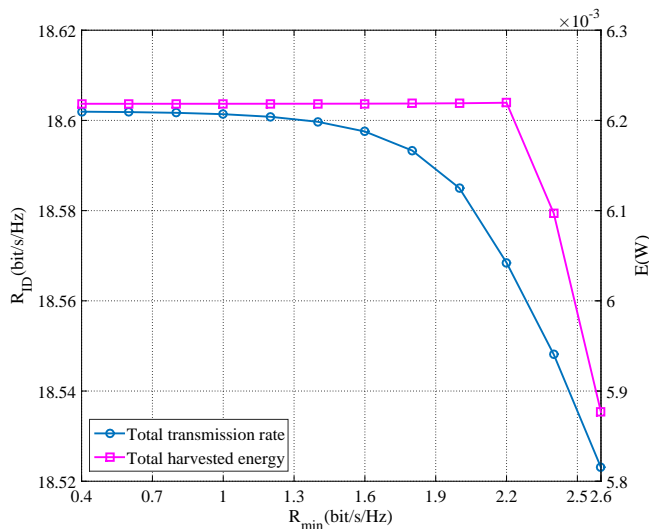


Fig. 8: Total transmission rate and harvested energy versus minimum transmission rate requirement with independent PS ratio.

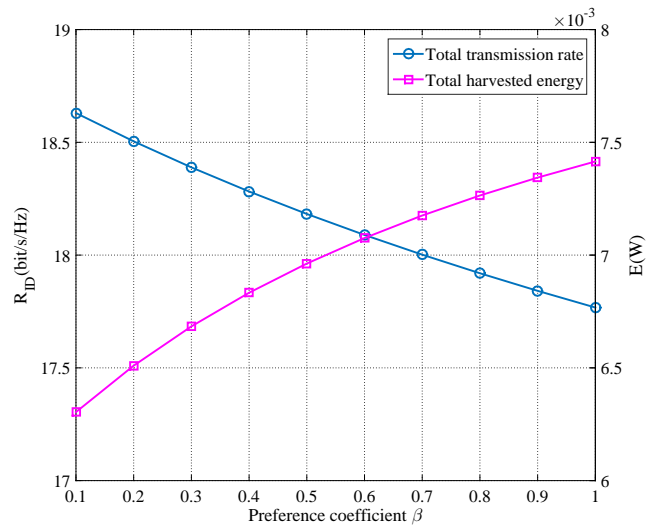


Fig. 10: Total transmission rate and harvested energy versus  $\beta$ .

transmission rate and the harvested energy constraints at each receiver. However, as  $R_{min}$  and  $E_{min}$  increase, the overall performance of the system needs to be compromised for the QoS of individual user. Taking the number of users into consideration, the maximum ESR is increasing with the number of users under the same QoS requirements, and this improvement becomes smaller with increasing users. This is attributed to the fact that the efficiency of EH enhances with the increasing number of users, and thus leads to a increasing ESR performance. On the other hand, more transmit power is needed to split to ID receivers so as to satisfy the increasing minimum rate requirements, and hence this improvement is limited by the rate requirements. In addition, the proposed algorithm with independent PS ratio outperforms the one with equal PS ratio, where the latter approach is less affected by the minimum rate requirement but decreases rapidly when the requirement of harvested energy enhances.

We further study the impact of minimum transmission rate and minimum harvested energy on the total transmission rate and the total harvested energy, respectively. As can be seen from Fig. 8, as  $R_{min}$  increases, the total transmission rate and the total harvested energy decrease sequentially. The reason is that as  $R_{min}$  increases, extra power is allocated to the first  $N - 1$  ‘weak’ users in order to meet their QoS demands, and hence less power is fed to the user with highest channel gain. The reduction of data rate of user with the best channel condition can not be compensated by the increasing rate from first  $N - 1$  users, thus degrades the system’s throughput. In addition, since more resources have been allocated for ID when  $R_{min}$  increases, the total harvested energy is also decreasing. On the contrary, the beneficial interference is fully utilized for EH without weakening the quality of data transmission. Fig. 9 shows that the total harvested energy increases with users’ minimum harvested energy  $E_{min}$ . Similarly, as  $E_{min}$

increases, the information transfer needs to be compromised for energy transfer, such that the total transmission rate decreases.

Finally, we analyse the impact of the preference parameter  $\beta$  to the transmission rate and harvested energy. The weighted factor  $\beta$  is used to control the service priority between ID (low  $\beta$ ) and EH (high  $\beta$ ). We consider the system involves six users with independent PS ratio. As it can be seen from Fig. 10, the result reveals that when the system gives priority to EH, more power is split to EH receiver and thus the total transmission rate decreases. Similarly, decreasing  $\beta$  leads to more weight putting on ID, such that the optimal direction of resource allocation is shifted to those obtained by maximizing the transmission rate. Therefore, it is very important for the decision maker to choose appropriate weights  $\beta$  according to the QoS requirements of the system.

## V. CONCLUSION

This paper investigates the joint optimization of the conflicting objectives on transmission rate and harvested energy for SWIPT NOMA systems. By considering the reverse link capacity as a function of the harvested energy and introducing a weighted coefficient, we transform the constrained MOO problem to a SOO problem. This non-convex problem is solved by decoupling it into two convex subproblems with iterative solution. Two algorithms are provided where the PS ratio at the receivers are optimized independently or equally. Numerical results demonstrate the improved ESR performance of the proposed strategy of jointly optimizing the power allocation and the PS ratio. More importantly, compared to the optimization only with respect to the transmission rate, our findings have illustrated that significant performance gain can be achieved by considering both transmission rate and harvested energy simultaneously. In addition, it has been shown in literature that the performance of NOMA cellular networks could be further improved with multi-carrier techniques, i.e., multi-carrier NOMA (MC-NOMA). Therefore, it is worthy of studying the joint subcarrier scheduling and resource allocation for SWIPT-based MC-NOMA cellular networks in the future.

## APPENDIX A

### PROOF OF PROPOSITION I

To prove *Proposition I*, we first analyze the second-order derivative of  $R(\mathbf{p})$  as (40). Thus, we arrive at the following conclusion

$$\frac{d^2 R(\mathbf{p})}{dp_a dp_b} = \begin{cases} \frac{d^2 R(\mathbf{p})}{dp_a^2}, & b > a; \\ \frac{d^2 R(\mathbf{p})}{dp_b^2}, & b < a. \end{cases} \quad (41)$$

Denoting  $\frac{d^2 R(\mathbf{p})}{dp_n^2}$  as  $w_n, n = 1, 2, \dots, N$ , the Hessian matrix of (31a) can be formulated as

$$\mathbf{H} = \begin{bmatrix} w_1 & w_1 & \cdots & w_1 \\ w_1 & w_2 & \cdots & w_2 \\ \vdots & \vdots & \ddots & \vdots \\ w_1 & w_2 & \cdots & w_N \end{bmatrix}, \quad (42)$$

where the  $n^{\text{th}}$  order principal minor of  $\mathbf{H}$  is

$$\begin{aligned} \mathbf{H}_n &= \begin{vmatrix} w_1 & w_1 & \cdots & w_1 \\ w_1 & w_2 & \cdots & w_2 \\ \vdots & \vdots & \ddots & \vdots \\ w_1 & w_2 & \cdots & w_n \end{vmatrix} \\ &= \begin{vmatrix} w_1 & w_1 & \cdots & w_1 \\ 0 & w_2 - w_1 & \cdots & w_2 - w_1 \\ \vdots & \vdots & \ddots & \vdots \\ 0 & 0 & \cdots & w_n - w_{n-1} \end{vmatrix} \\ &= w_1 \prod_{i=2}^n (w_i - w_{i-1}) \quad \forall n = 1, 2, \dots, N, \end{aligned} \quad (43)$$

It's obvious that  $\mathbf{H}_1 < 0$  for the case of  $w_1 < 0$ . When  $2 \leq n \leq N$ , we can write  $w_i - w_{i-1}$  as (44).

To prove that the equivalent-sum-rate  $R(\mathbf{p})$  is a concave function with respect to  $\mathbf{p}$ , the matrix  $\mathbf{H}$  should be negative semi-definite. Equivalently  $\mathbf{H}_n \leq 0$  when  $n$  is odd and  $\mathbf{H}_n \geq 0$  when  $n$  is even, which can be achieved if and only if  $w_i - w_{i-1} \leq 0$  holds for all  $n = 2, 3, \dots, N$ . As a result,  $\rho_1 |h_1|^2 \leq \rho_2 |h_2|^2 \leq \dots \leq \rho_N |h_N|^2$  is the necessary and sufficient condition. This completes the proof. ■

## REFERENCES

- [1] H. Zhang, Y. Dong, J. Cheng, M. J. Hossain, and V. C. M. Leung, "Fronthauling for 5G LTE-U ultra dense cloud small cell networks," *IEEE Wireless Commun.*, vol. 23, no. 6, pp. 48 – 53, Dec. 2016.
- [2] Z. Ding, X. Lei, G. K. Karagiannidis, R. Schober, J. Yuan, and V. Bhargava, "A survey on non-orthogonal multiple access for 5G networks: Research challenges and future trends," *IEEE Journal Sel. Areas Commun.*, vol. 35, no. 10, pp. 2181–2195, Oct. 2017.
- [3] Z. Chen, Z. Ding, X. Dai, and R. Zhang, "An optimization perspective of the superiority of NOMA compared to conventional OMA," *IEEE Trans. Sig. Process.*, vol. 65, no. 19, pp. 5191–5202, Oct. 2017.
- [4] Z. Yong, V. W. S. Wong, and R. Schober, "Stable throughput regions of opportunistic NOMA and cooperative NOMA with full-duplex relaying," *IEEE Trans. Wireless Commun.*, vol. 17, no. 8, pp. 5059–5075, Aug. 2018.
- [5] Z. Ding, P. Fan, and H. V. Poor, "Impact of user pairing on 5G non-orthogonal multiple-access downlink transmissions," *IEEE Trans. Veh. Techn.*, vol. 65, no. 8, pp. 6010–6023, Aug. 2016.
- [6] F. Fang, H. Zhang, J. Cheng, S. Roy, and V. C. M. Leung, "Joint user scheduling and power allocation optimization for energy efficient NOMA systems with imperfect CSI," *IEEE Journal Sel. Areas Commun.*, vol. 35, no. 12, pp. 2874–2885, Dec. 2017.
- [7] L. Fan, X. Lei, Y. Nan, T. Q. Duong, and G. K. Karagiannidis, "Secure multiple amplify-and-forward relaying with co-channel interference," *IEEE Journal Sel. Topics Sig. Proc.*, vol. 10, no. 8, pp. 1494–1505, Dec. 2016.
- [8] L. Fan, Z. Rui, F. K. Gong, Y. Nan, and G. Karagiannidis, "Secure multiple amplify-and-forward relaying over correlated fading channels," *IEEE Trans. Wireless Commun.*, vol. 65, no. 7, pp. 2811–2820, July 2017.
- [9] H. Zhang, N. Yang, K. Long, M. Pan, G. K. Karagiannidis, and V. C. M. Leung, "Secure communications in NOMA system: Subcarrier assignment and power allocation," *IEEE Journal Sel. Areas Commun.*, vol. 36, no. 7, pp. 1441–1452, July 2018.
- [10] Y. Chi, L. Lei, G. Song, C. Yuen, L. G. Yong, and L. Ying, "Practical MIMO-NOMA: Low complexity capacity-approaching solution," *IEEE Trans. Wireless Commun.*, vol. 17, no. 9, pp. 6251–6264, Sept. 2018.
- [11] M. N. Kulkarni, A. Ghosh, and J. G. Andrews, "A comparison of MIMO techniques in downlink millimeter wave cellular networks with hybrid beamforming," *IEEE Trans. Commun.*, vol. 64, no. 5, pp. 1952–1967, May 2016.
- [12] F. Wang, J. Xu, and Z. Ding, "Optimized Multiuser Computation Offloading with Multi-antenna NOMA," in *IEEE Globecom Workshops (GC Wkshps)*, 2017, pp. 1–7.

$$\begin{aligned} \frac{d^2 R(\mathbf{p})}{dp_a dp_b} &= \frac{d^2(R_{ID}(\mathbf{p}) + \beta R_{EH}(\mathbf{p}))}{dp_a dp_b} = \frac{d^2 R_{ID}(\mathbf{p})}{dp_a dp_b} \\ &= \frac{-\rho_1^2 |h_1|^4}{\ln 2 (\rho_1 |h_1|^2 \sum_{i=1}^N p_i + \sigma^2)^2} + \sum_{n=1}^{a-1} \left( \frac{\rho_n^2 |h_n|^4}{\ln 2 (\rho_n |h_n|^2 \sum_{i=n+1}^N p_i + \sigma^2)^2} - \frac{\rho_{n+1}^2 |h_{n+1}|^4}{\ln 2 (\rho_{n+1} |h_{n+1}|^2 \sum_{i=n+1}^N p_i + \sigma^2)^2} \right) \end{aligned} \quad (40)$$

$\forall a, b = 1, 2, \dots, N.$

$$\begin{aligned} w_i - w_{i-1} &= \frac{\rho_{n-1}^2 |h_{n-1}|^4}{\ln 2 (\rho_{n-1} |h_{n-1}|^2 \sum_{i=n}^N p_i + \sigma^2)^2} - \frac{\rho_n^2 |h_n|^4}{\ln 2 (\rho_n |h_n|^2 \sum_{i=n}^N p_i + \sigma^2)^2} \\ &= \frac{2\rho_{n-1}\rho_n |h_{n-1}|^2 |h_n|^2 \sum_{i=n}^N p_i \sigma^2 + (\rho_{n-1} |h_{n-1}|^2 + \rho_n |h_n|^2) \sigma^4}{\ln 2 (\rho_{n-1} |h_{n-1}|^2 \sum_{i=n}^N p_i + \sigma^2)^2 (\rho_n |h_n|^2 \sum_{i=n}^N p_i + \sigma^2)^2} (\rho_{n-1} |h_{n-1}|^2 - \rho_n |h_n|^2) \end{aligned} \quad (44)$$

- [13] W. Lu, Y. Gong, X. Liu, J. Wu, and H. Peng, "Collaborative energy and information transfer in green wireless sensor networks for smart cities," *IEEE Trans. Industrial Informatics*, vol. 14, no. 4, pp. 1585–1593, April 2018.
- [14] X. Lu, P. Wang, D. Niyato, D. I. Kim, and Z. Han, "Wireless networks with RF energy harvesting: A contemporary survey," *IEEE Communications Surveys & Tutorials*, vol. 17, no. 2, pp. 757–789, 2015.
- [15] L. R. Varshney, "Transporting information and energy simultaneously," in *IEEE Int. Symp. Inf. Theory*, 2008, pp. 1612–1616.
- [16] R. Zhang and C. K. Ho, "MIMO broadcasting for simultaneous wireless information and power transfer," *IEEE Trans. Wireless Commun.*, vol. 12, no. 5, pp. 1989–2001, May 2013.
- [17] Y. Hu, Y. Zhu, M. C. Gursoy, and A. Schmeink, "SWIPT-enabled relaying in IoT networks operating with finite blocklength codes," *IEEE Journal Sel. Areas Commun.*, vol. 37, no. 1, pp. 74–88, Jan. 2019.
- [18] W. Lu, Y. Gong, J. Wu, H. Peng, and J. Hua, "Simultaneous wireless information and power transfer based on joint subcarrier and power allocation in OFDM systems," *IEEE Access*, vol. 5, pp. 2763–2770, Feb. 2017.
- [19] N. Janatian, I. Stupia, and L. Vandendorpe, "Multi-objective resource allocation optimization for SWIPT in small-cell networks," in *Wireless Information and Power Transfer: A New Paradigm for Green Communications*. Springer, 2018, pp. 65–86.
- [20] S. K. T. O. Seokju Jang, Hoon Lee and I. Lee, "Energy Efficient SWIPT systems in multi-cell MISO networks," *IEEE Trans. Wireless Commun.*, vol. 17, no. 12, pp. 8180–8194, Dec. 2018.
- [21] Z. Xiang and Q. Li, "Energy Efficient for SWIPT in MIMO two-way amplify-and-forward relay networks," *IEEE Trans. on Veh. Technol.*, vol. 67, no. 6, pp. 4910–4924, June 2018.
- [22] W. Lu, T. Nan, Y. Gong, M. Qin, X. Liu, Z. Xu, and Z. Na, "Joint resource allocation for wireless energy harvesting enabled cognitive sensor networks," *IEEE Access*, vol. 6, pp. 22480–22488, April 2018.
- [23] P. D. Diamantoulakis, K. N. Pappi, Z. Ding, and G. K. Karagiannidis, "Wireless-powered communications with non-orthogonal multiple access," *IEEE Trans. Wireless Commun.*, vol. 15, no. 12, pp. 8422–8436, Dec. 2016.
- [24] P. D. Diamantoulakis, K. N. Pappi, G. K. Karagiannidis, X. Hong, and A. Nallanathan, "Joint downlink/uplink design for wireless powered networks with interference," *IEEE Access*, vol. 5, no. 99, pp. 1534–1547, Jan. 2017.
- [25] Y. Xu, C. Shen, Z. Ding, X. Sun, S. Yan, G. Zhu, and Z. Zhong, "Joint beamforming and power-splitting control in downlink cooperative SWIPT NOMA systems," *IEEE Trans. Sig. Process.*, vol. 65, no. 18, pp. 4874–4886, Sept. 2017.
- [26] T. N. Do, D. B. D. Costa, T. Q. Duong, and B. An, "Improving the performance of cell-edge users in MISO-NOMA systems using TAS and SWIPT-based cooperative transmissions," *IEEE Trans. Green Commun. Networking*, vol. 2, no. 1, pp. 49–62, March 2018.
- [27] H. Sun, F. Zhou, R. Q. Hu, and L. Hanzo, "Robust beamforming design in a NOMA cognitive radio network relying on SWIPT," *IEEE Journal Sel. Areas Commun.*, vol. 37, no. 1, pp. 142–155, Jan. 2019.
- [28] M. P. Linglong Dai, Bichai Wang and S. Chen, "Hybrid precoding-based millimeter-wave massive MIMO-NOMA with simultaneous wireless information and power transfer," *IEEE Journal Sel. Areas Commun.*, vol. 37, no. 1, pp. 131–141, Jan. 2019.
- [29] Y. Saito, A. Benjebbour, Y. Kishiyama, and T. Nakamura, "System-level performance evaluation of downlink non-orthogonal multiple access (NOMA)," in *IEEE International Symposium on Personal Indoor Mobile Radio Communications (PIMRC)*, 2013.
- [30] Z. Ding, Z. Yang, P. Fan, and H. V. Poor, "On the performance of non-orthogonal multiple access in 5G systems with randomly deployed users," *IEEE Signal Processing Letters*, vol. 21, no. 12, pp. 1501–1505, Dec. 2014.
- [31] E. Bjornson, E. A. Jorswieck, M. Debbah, and B. Ottersten, "Multi-objective signal processing optimization: The way to balance conflicting metrics in 5G systems," *IEEE Sig. Process. Mag.*, vol. 31, no. 6, pp. 14–23, Nov. 2014.
- [32] J. Tang, D. K. C. So, E. Alsusa, and K. A. Hamdi, "Resource efficiency: A new paradigm on energy efficiency and spectral efficiency tradeoff," *IEEE Trans. Wireless Commun.*, vol. 13, no. 8, pp. 4656–4669, Aug. 2014.
- [33] G. B. L. C. A. C. Coello and D. A. V. Veldhuizen, *Evolutionary Algorithms for Solving Multi-Objective Problems*. New York: Springer, 2007.
- [34] Z. Yang, W. Xu, C. Pan, Y. Pan, and M. Chen, "On the optimality of power allocation for NOMA downlinks with individual QoS constraints," *IEEE Commun. Lett.*, vol. 21, no. 7, pp. 1649–1652, July 2017.
- [35] S. Boyd and L. Vandenberghe, *Convex Optimization*. Cambridge University Press, Cambridge, UK, 2004.
- [36] X. Huang and V. Y. Pan, "Fast rectangular matrix multiplication and applications," *Journal of Complexity*, vol. 14, no. 2, pp. 257 – 299, 1998. [Online]. Available: <http://www.sciencedirect.com/science/article/pii/S0885064X98904769>
- [37] GreenTouch, *Mobile Communications WG architecture doc2: Reference scenarios*, May. 2013.
- [38] Y. Huang, M. Liu, and L. Yuan, "Energy-efficient SWIPT in IoT distributed antenna systems," *IEEE Internet of Things Journal*, vol. 5, no. 4, pp. 2646–2656, Aug. 2018.
- [39] X. Zhou, R. Zhang, and C. K. Ho, "Wireless information and power transfer in multiuser OFDM systems," *IEEE Trans. Wireless Commun.*, vol. 13, no. 4, pp. 2282–2294, April 2014.